International Journal of Oil, Gas and Coal Engineering
2024; 12(1): 10-19
http://www.sciencepublishinggroup.com/j/ogce
doi: 10.11648/j.ogce.20241201.12
ISSN: 2376-7669 (Print); ISSN: 2376-7677 (Online)

Integrated Petrophysical and Petrographical Studies for Reservoir Characterization: A Case Study of the Khmer Basin in Cambodian Water, Gulf of Thailand

Kimhak Neak[1, 2, *], Kakda Kret[1, 3], Tola Sreu[3], Sirisokha Seang[3], Sokunthea Khoun[2], Chanmoly Or[1, 3]

[1]Research and Innovation Centre, Institute of Technology of Cambodia, Phnom Penh, Cambodia

[2]General Department of Petroleum, Ministry of Mines and Energy, Phnom Penh, Cambodia

[3]Faculty of Geo-Resource and Geotechnical Engineering, Institute of Technology of Cambodia, Russian Federation Blvd., Phnom Penh, Cambodia

Email address:

kimhakneak@gmail.com (Kimhak Neak)

[*]Corresponding author

To cite this article:

Kimhak Neak, Kakda Kret, Tola Sreu, Sirisokha Seang, Sokunthea Khoun et al. (2024). Integrated Petrophysical and Petrographical Studies for Reservoir Characterization: A Case Study of the Khmer Basin in Cambodian Water, Gulf of Thailand. *International Journal of Oil, Gas and Coal Engineering*, *12*(1), 10-19. https://doi.org/10.11648/j.ogce.20241201.12

Received: November 30, 2023; **Accepted**: December 26, 2023; **Published**: January 11, 2024

Abstract: The Khmer Basin is one of the sedimentary basins in the Gulf of Thailand (GoT). This basin is located in the central east of the gulf, about 180 km from the Cambodian coastal baseline and an average of 80 m water depth in offshore Cambodia. It is an elongated N-S trending rift basin that extends 150 km in length and 60 km in width. Even though a high potential hydrocarbon accumulation reservoir was discovered in the late nineteenth century, the Apsara oil field in the northeast of the basin just started producing the first oil for Cambodia in late 2020 by KrisEnergy. However, there are a small number of publications about the Khmer Basin compared to the Pattani Basin to the west and the Malay Basin to the south. This study aims to identify the textures of the sedimentary grain, mineralogy, and diagenesis process of sandstone reservoirs which correspond to the quality of porosity and permeability in the confined layers from the Oligocene to Middle Miocene age. The core samples of the exploration well, Apsara-1 (1993), were provided by the General Department of Petroleum (GDP), Ministry of Mines and Energy (MME) for the purposes of academics. Thin section and SEM microscopic image analysis are applied to assist this petrographic study to observe the rock components and the relationship of grains and matrix, cementation and the diagenetic processes. X-ray diffractometer (XRD) is used to determine the mineral compositions and clay minerals. X-ray Fluorescence (XRF) is used to evaluate major oxide concentrations in reservoir intervals. The stratigraphy in a section, ranging from 2776 m to 2781 m consists of sandstones interbedding with shales and coals. Mudstones which are composed of silt shale and coal appear in dark-grey to black thin layers in the study section. The porosity of the sample determines the diverse pore spaces in the reservoir sand, ranging under 12%. The data analysis, the clastic, pore geometry, buried compaction, diageneses and fractures impact relatively on reservoir quality. The porosity reduction is directly influenced by mechanical compaction, quartz overgrowth, the pore fillings by detrital clays and mineral replacement.

Keywords: Apsara Oil Field, Khmer Basin, Pattani Basin, Sandstone Reservoir, Reservoir Quality and Diagenesis

1. Introduction

The Khmer Basin was first known as the Khmer Trough since the earlier explorations of oil and gas resources were conducted in the Khmer Shelf, gulf of Thailand (GoT). Elf/Esso and Marine Associate/Canadian Reserves were the two major teams that were officially granted the first exploration licenses from the Royal Government of Cambodia for hydrocarbon resources exploration in offshore Cambodia [1]. During 1970 – 1974 Elf/Esso acquired and shot a huge number of 2D seismic lines in the acreage and concluded to

drill 3 exploration wells, these wells were reported as tight and dry holes [2, 3].

After a civil war in the country, Russian and Cambodian geologists conducted geological and geophysical investigations (a regional grid of seismic lines) and illustrated the mapping of sedimentary basins in the country, including the Cambodian territorial sea area where the licenses were divided into 7 offshore blocks (Block I – VII) [2, 4]. From 1992 – 1998, there have been done 2D, 3D, and well drilling by various companies, such as Enterprise (Block I & II), Campex (Block III), and Premier (Block IV). These four companies found different successes which indicated the presence of oil and gas for a possible economic [2, 3, 5].

In 1998, all these four companies decided to leave their block license when global oil prices slumped lower. One year later, Woodside entered into a study agreement with the government to determine the prospective of those Blocks and the feasibility of developing the discovered reserves [2, 4, 6]. As a result, in 2002, the Royal Government of Cambodia revised the offshore blocks from Arabic Numbers (I – VII) to alphabets (A – F), thereof, area A (as shown in Figure 1) was demarcated based on a high potential prospect of the emerging western parts of previous Block I, II, III and IV.

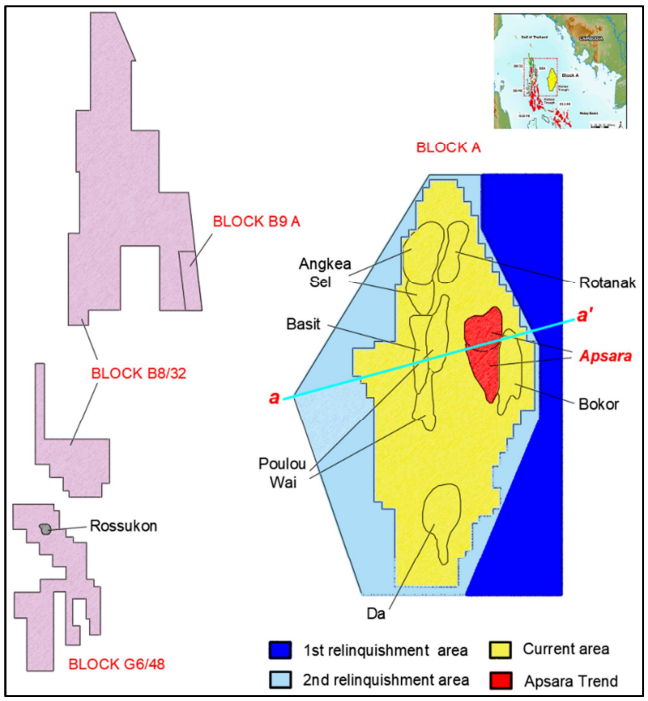

Figure 1. *Seven geological trends in the CBA. Red areas are the Apsara oil fiend where KrisEnergy launched a Mini Phase 1A to produce the first oil of Cambodia, after Kimhak et al., (2023).*

A joint venture of Chevron Texaco and Moeco signed a production sharing contract (PSC) with the government to explore and appraise wells in area A (Cambodian Block A, CBA) in 2002. The operator of CBA confirmed the presence of hydrocarbons with light and sweet crude oils in various geological trends, particularly the Apsara trend in the Phimean Akas Area, in the north-eastern center of the body of the Khmer Basin [4, 7, 8].

KrisEnergy afterward became the major operator of the CBA in 2014 when Chevron was not able to reach an agreement with the Royal Government of Cambodia on revenue sharing of oil production profit. The attempt to produce the first oil for the country was successful in late 2020 when KrisEnergy launched a Mini Phase 1A with a minimum facilities wellhead support structure capable of housing up to six development wells. The pilot oil-producing project seemed to test the proven reservoir whether it could be expanded to a broader production in the future, yet it was underperformance that resulted in stopped production after six months [9, 10].

The production targets of both Chevron and KrisEnergy was based on sand bodies in age of Upper Oligocene to Middle Miocene in Apsara geological trend where is the most prospective oil and gas to be extracted [7, 11, 12].

The geological formation of the Khmer Basin, consisting of the CBA, in the GoT is reported many similarities to other Thai, Malaysian and Vietnamese Basin which lie to the west, south and east respectively. Geological characteristics including age and type of source rock, age and type of reservoir rocks, structural trapping styles and the hydrocarbon reservoirs are extremely complexities and uncertainties. The quality of reservoirs in fine-grained clastic rocks is influenced by various interconnected factors, including pore water chemistry, mineral composition, thermal gradient, diagenetic events, formation pressure, burial depth, subsurface structures and depositional environment. This study aims to identify the texture of the sedimentary grain, mineralogy, and diagenesis process of sandstone reservoirs which correspond to the quality of porosity and permeability in the confined layers from the Oligocene to Middle Miocene age in Apsara oil field through core samples which were drilled by Campex in 1993.

2. Methodology

A total of six sandstone samples which are from a five meters section of a reservoir layer of an exploration well Apsara-1 (Figure 2) were subjected to X-ray fluorescence (XRF), Petrographic Microscopy, X-ray Diffraction (XRD) and Scanning Electron Microscopy (SEM) analyses. The XRF analysis was carried out at the Institute of Technology of Cambodia, Phnom Penh, Cambodia. The samples were milled to less than 50 µm in size and pressed pellets were prepared. The pressed pellets were analyzed for the major oxides using a PANalytical Zetium XRF spectrometer equipped with a 4kWRh tube. The milled samples were also dried at 100°C and heated at 1000 ˚C for a period of at least 3 h to oxidize sulfur (S) and iron (Fe2+) to determine the oxide elements and the loss of ignition (LOI).

Petrographic Microscopy of thin-section analysis was used to determine mineralogical compositions, textural characteristics and cementations. The grain size distribution of the sandstone was counted by Fiji Application software through grain visuals. The grain-contact pore, grain shapes and grain shorting were also primarily observed to access the quality of the medium to store and flow the reservoir fluids. Six samples were analyzed by XRD to determine the mineral

composition of the sandstone, especially mineral clay cementations in the grain coating and pore filling. Microstructures of clay species, micropore geometry, and pore material precipitations were observed by SEM analysis to identify the major factors of diagenesis to reduce primary porosity.

In addition, the Helium gas flow porosity and Klinkenberg permeability were also measured to correlate with the pores of the micrograph images.

3. Lithostratigraphy

Khmer Basin commenced and developed relatively with the formation of the Gulf of Thailand (GoT). The initiation of basin formation probably commenced as early as in Eocene, coinciding with the collision of the Indian Plate with the Eurasian Plate that led to form a series of strike-slip faults through the GoT, including the Three Pagodas Fault Zone (TPFZ), the Kho Samui Fault (KSF), and their conjugates the Khlong Marui Fault (KMF) and the Ranong Fault. The extension and crustal thinning under the GoT related to the strike-slip faults of tectonic movements in the region of Indochina to form the Khmer Basin in a similar way as the Pattani, Malay and other Tertiary Basins in the GoT [5, 13, 14].

The Basin is located in central east of the Gulf of Thailand, separated from Pattani Basin in Thai water to the west by Narathiwat Ridge, from North Malay Basin in Peninsular water by Kim Qui High to the south and was directly influenced by TPFZ in the north [13, 15]. Khmer Basin is one of the sub-basins which occurs as an N-S elongate rift basin in the GoT associated with Eocene/Oligocene oblique slip and extends a length and width of 150 km and 60 km respectively.

This Tertiary basin buried the sediments in various depositional environments at a depth up to 8 km in the central part of the basin [3, 16]. Typical sedimentology developments in the Eocene to Late Oligocene were the fluvial/alluvial to fluvial lacustrine sediments in the Syn-rift phase. From Lower Miocene to Plio-Pleistocene basin sediments were reflected to the fluvial, marine/fluvial and marine sediments which progressed in the post-rift phase, as shown in Figure 2 [4, 11, 17].

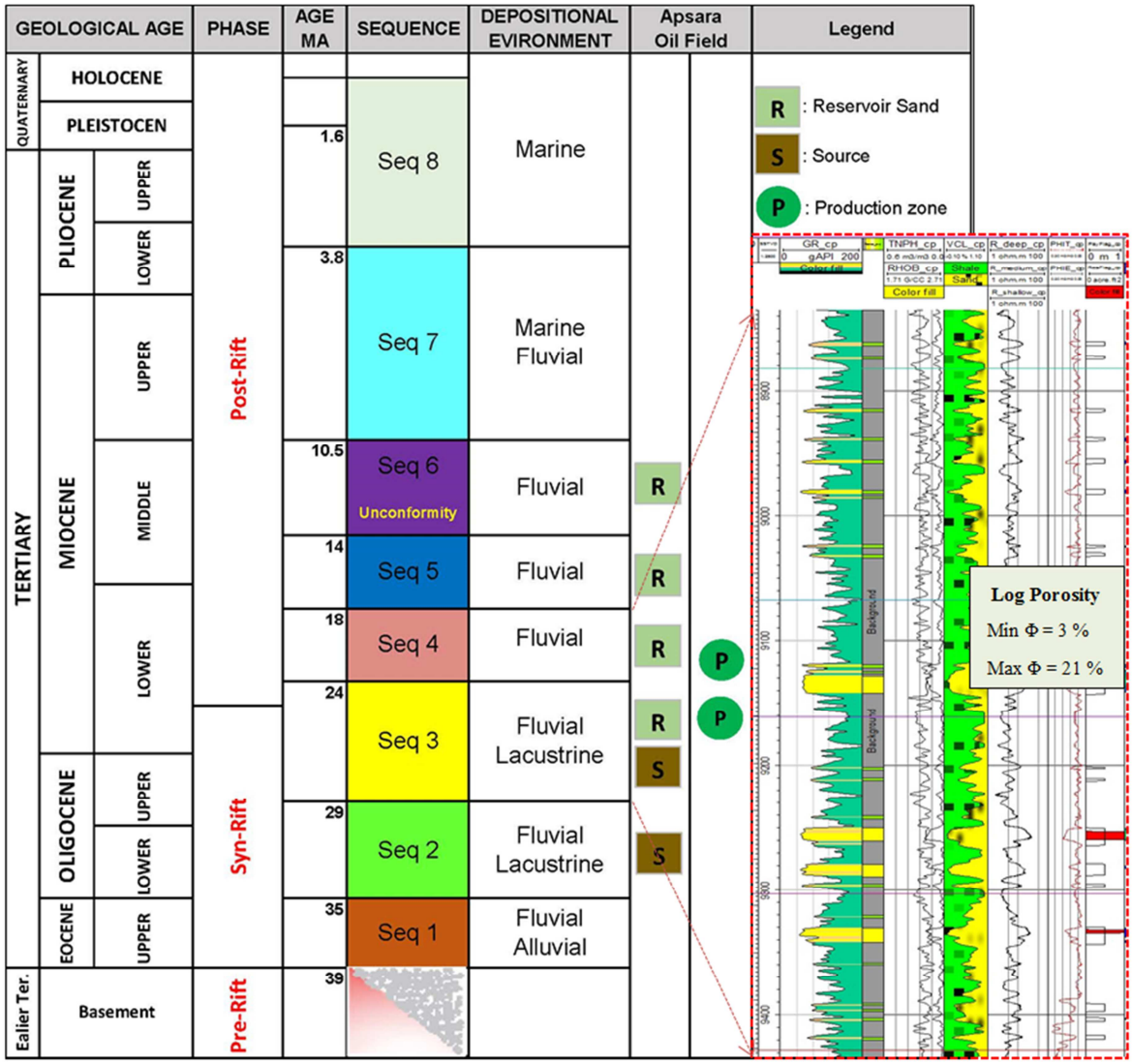

Figure 2. *The Khmer Basin stratigraphy sequence correlations with tectonic processes and lithology loggings (provided by GDP).*

The sediment deposition in the Khmer Basin is subdivided into 8 sequential strata, sequence 1 is the oldest deposit at the bottom and sequence 8 is the youngest at the top.

Sequences 1–3 are in syn-rift deposits comprised of alluvial, fluvial and lacustrine sediments. Lacustrine shales are present in these syn-rift sequences, some of which are sources for the oil and gas accumulations in the Khmer Basin. Most known hydrocarbon-bearing reservoirs within the Khmer Basin belong to the latest syn-rift to post-rift, lower Miocene fluvial-lacustrine and fluvial sandstones in Sequences 3 and 4. Sequences 5 and 6 are dominantly fluvial, which potentially can be additional hydrocarbon-bearing reservoirs, as shown in Figure 2 [11, 17].

4. Hydrocarbon Reservoir

The potential petroleum system of the Khmer Basin has many similarities to the adjacent oil and gas producing reservoirs in the Pattani Basin including source rock, age, trapping style and rock types [18, 19]. The Upper Oligocene lacustrine represents the primary source for liquid hydrocarbons in sequence 3. Miocene coaly and shallow lacustrine sediments also significantly generated light oil and gas/condensate systems in sequence 4 [11, 18].

Structural closures in the Khmer Basin are mainly 3-way dip-fault structures situated within a series of north-south trending fault blocks [11, 17].

The commercial reservoir section of the Khmer Basin is an alternating sequence of sand and shale with a few local coals in the complex formation from the top of sequence 3 to sequence 4, as seen in Figure 2. Most of the reservoir sections were deposited in a fluvial/coastal plain environment, with linear, discontinuous sands through laterally extensive amalgamated sand sequences.

The oil pay in both sequences ranges in the true vertical depth of 2130 m to 2910 m and the temperature is ranging from 125˚C to 163˚C. Sequence 4 sands tend to be thicker and stacked by amalgamated channels, whereas those of Sequence 3 are thinner, and formed from isolated channels [4, 11, 17].

Figure 3 (a) is a sequential stratigraphical correlation from East to West across early exploration wells, Devada-1 and Apsara-1 which were drilled in the 1990s. A green dot which is located above the middle of the sediment thickness of sequence 3–4, indicate reservoir section in the Apsara oil field area and the availability of the core sample for the study in this paper. Core Ap-2 was taken to analyze petrophysical and petrographical properties including thin-section, SEM, XRF, XRD, porosity and permeability.

Sedimentological features were observed through five core boxes, continuing the depth in the reservoir sandstone interbedded with shale and siltstone from 2776 to 2781 m.

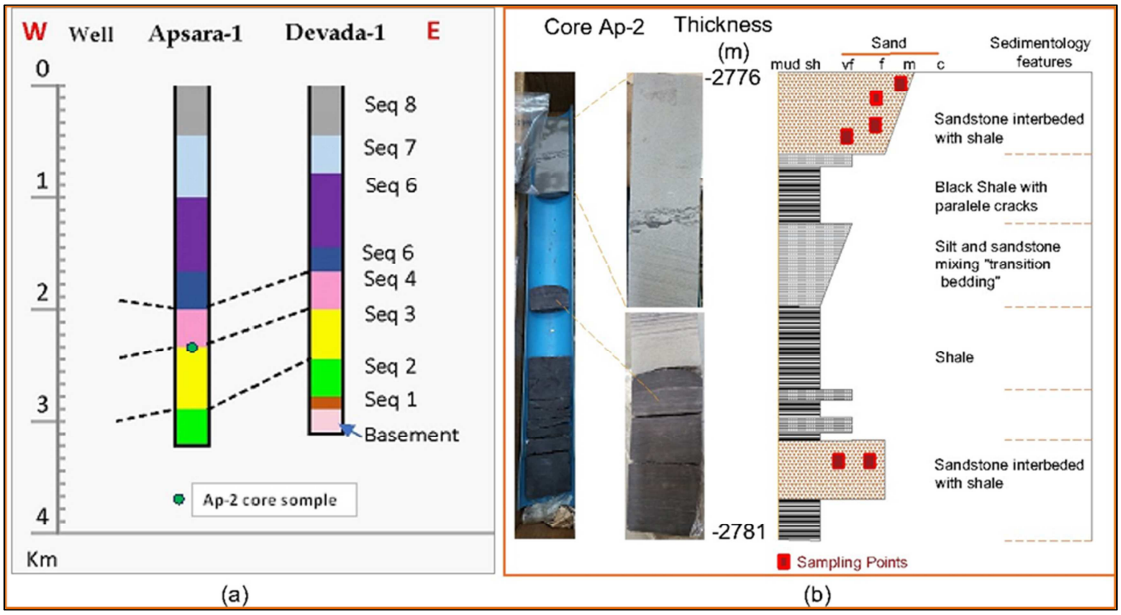

Figure 3. *Campex drilled an explorational well (Apsara-1, 1993) in Phimean Akas (PA) area where Cambodian first oil is produced. (a) Sequential strata correlation with depth and thickness, and the indication of available core samples for this study; (b) Sedimentological features at the depth of 2776 – 2781 m.*

5. Results and Discussions

5.1. Sedimentological Features

The length of 5 m of these five core boxes could be observed the interbedding layers of sand and silty shale with occasional coals and classified in sandstone, shale and silt as the rock type by visible appearances. The first body of sandstone was a coarsening upward sandstone layer consisting fine to medium grain size. Siltstones comprise of muds to very fine textural grain which were observed in thin dark grey layers. Silty rock layers seem to be a transition zone of textural grain of sand to clayey shale.

5.2. Petrography of Sandstone Reservoir

The polish section images describe that the sandstone is

composed of detrital constituents, pores, matrixes, minerals, and cement [20]. In Figure 4 (a-b), the detrital constituents consist of quartz, plagioclase feldspar, calcite, and diverse lithic fragments which correspond to the grain size distribution from silty clay to medium sand grain, sizing up to 288 µm. Most of the Quartz and Plagioclase feldspar grains fall in the range of very fine to fine grains, 64 to 160 µm, and fewer grains are in the range of 161 to 288 µm, as shown in Figure 4 (e). The framework grains illustrate the inadequately to moderately sorted grains, occasionally containing pebbles, with subangular to subrounded shapes, and complex packing styles.

The image analysis observation could notice the pore systems into two significant pore types, (1) the pore space between grain-grain contacts, and (2) the pore space of grain dissolutions, and there might be the additional pore of grain fracture pore space which could potentially contribute the total pore in the rock body.

The matrixes are situated in the spaces of grain-grain connections since the beginning of sediment accumulation in the typical depositional environment. These matrixes occasionally became the strong lithic cementation that surrounded the framework grain as seen in the deep black texture, shown in Figure 4 (a) and (b). The cement and mineral clays are the material that occurred after the deposition of the clastic sediments and are situated at the coating of the detrital grains, shown specifically in the grain-grain contact spaces. Calcite minerals could be recognized through the polish section image modes which are the calcite cement and detrital replacement grains, the zigzag boundary [21].

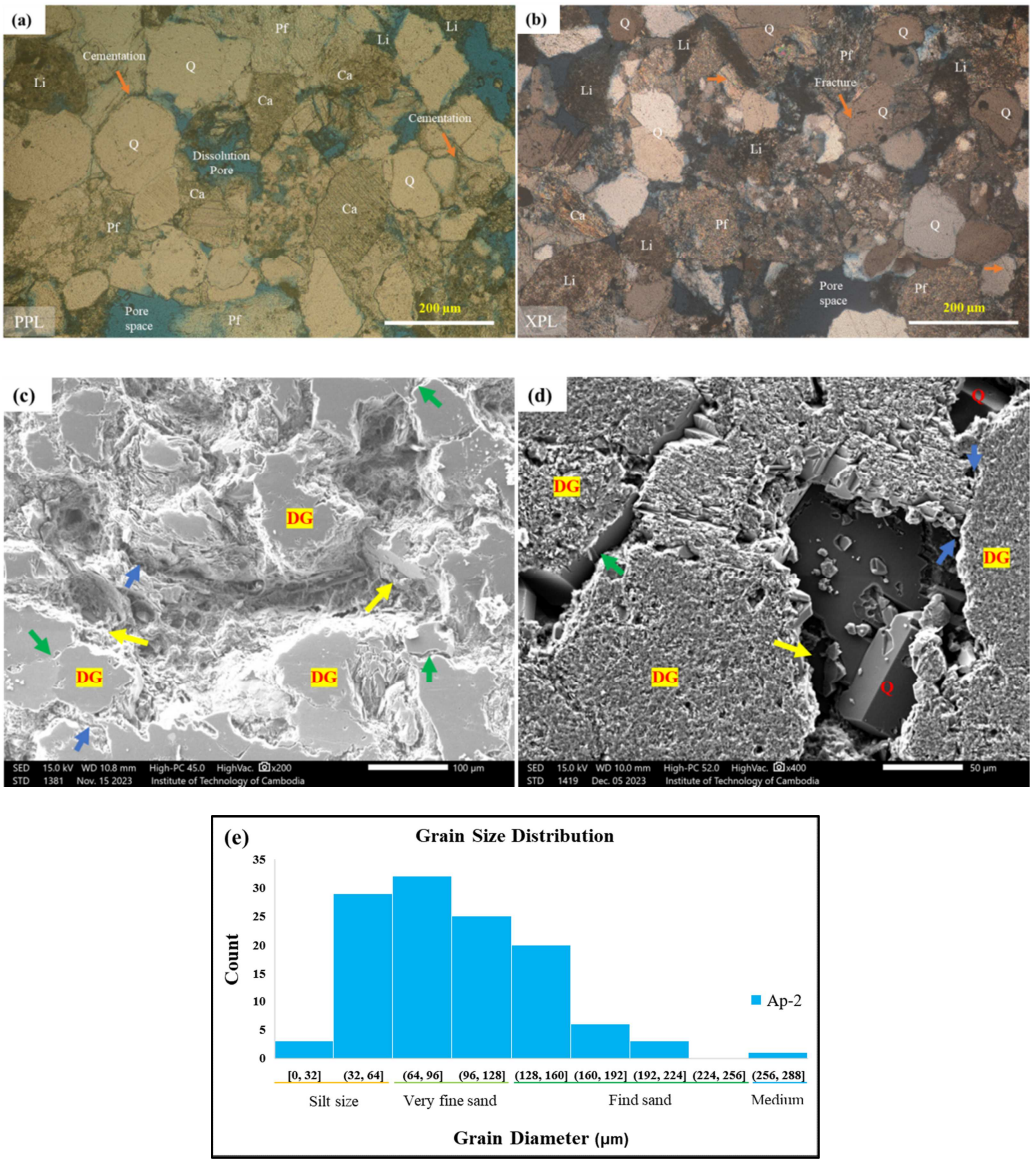

Figure 4. *Optical images of the sandstone reservoir at the depth of 2776 - 2781 m, Apsara-1 (1993) reveal the rock compositions and rock textures by polish sections and SEM analysis, Q: Quartz, Li: Lithic fragment, Pf: Plagioclase feldspar, Ca: Calcite and DG: Detrital grain. (a), the polish section image in PPL mode indicates the grain minerals, pore systems, and cement-grain boundary; (b), the image of the different samples shows the changes of grain mineral color in XPL mode, indicating the additional information of the mineral boundary, fracture, pore throat, and detrital connection; (c), the major pore networks at the most porous rock surface, showing larger intergranular pores, pore throats, micropore and clay cement; (d), minor pore system at the grain-grain contacts and quartz overgrowth replacement; (e), the grain size of distribution of the sandstone reservoir in the section.*

The SEM image, as seen in Figure 4 (c), captured the detailed fraction of rock components in the most porous surface of the sample plate. The major pore networks are huge and irregular connections that link the pore throats of grain-grain contact pores (green arrow) to grain-dissolution pores. Clay minerals are growing in every pore type, in the form of grain coatings, authigenic grain, and mineral precipitations (yellow arrow).

Figure 4 (d) shows the SEM image of the microstructure of the sandstone reservoir sample at a poor porosity surface. Most of these typical structures are observed at the lithic fragment spot which indicates the pore seams of grain-grain boundary (green arrow), porous structures grain and mineral overgrowth pore fillings (quartz). In general, the micropore network seems to connect well through the narrow space of mineral crystallizations, as seen in the blue arrows.

5.3. Geochemical and Mineralogy

5.3.1. Major Oxide Concentration

The major oxides of the sandstone reservoir are presented in the *Table 1*. The compositions built on the rock are predominantly SiO_2 which ranges the concentration of oxides from 49.99 % to 65.22 %, followed by Al_2O_3, Fe_2O_3, MgO and K_2O range from 4.97 % to 9.70 %, 1.68 % to 3.34 %, 1.65 % to 2.47 % and 0.78 % to 1.74 % respectively. The other minor oxide elements are lower fractions such as MnO, TiO_2, Na_2O and P_2O_5.

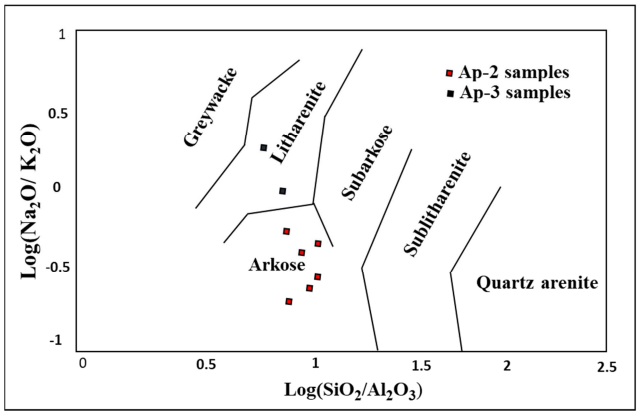

Figure 5. *Chemical classification of Miocene sandstone reservoir in the Phi Mean Akas Area based on Log(SiO_2/Al_2O_3) versus Log(Na_2O/K_2O) is plotted in the field of arkose, (after Pettijohn et al., 1972).*

Table 1. *Results of oxide concentration (wt%) analyzed by X-ray fluorescence.*

Depth (m)	2776	2781	2777	2961	2963
Rock	**Arkose**	**Arkose**	**Arkose**	**Arkose**	**Arkose**
SiO_2 (%)	56.09	65.22	57.46	49.99	58.54
TiO_2 (%)	0.41	0.32	0.21	0.21	0.52
Al_2O_3 (%)	8.15	8.54	6.04	4.97	9.7
Fe_2O_3 (%)	2.76	2.62	1.68	2.17	3.34
MnO (%)	0.15	0.06	0.13	0.24	0.12
MgO (%)	2.29	2.15	1.65	2.14	2.47
CaO (%)	13.99	9.44	16.46	19.97	10.48
Na_2O (%)	0.44	0.78	0.48	0.38	0.45
K_2O (%)	1.41	1.34	0.91	0.78	1.74
P_2O_5 (%)	0.08	0.07	0.05	0.07	0.11
LOI	13.25	9.61	14.4	17.13	11.37
Total	99.01	100.15	99.47	98.05	98.84
Log (SiO_2/Al_2O_3)	0.84	0.88	0.98	1	0.78
Log (Na_2O/K_2O)	-0.51	-0.24	-0.28	-0.31	-0.59

The study sandstone was classified according to the scheme proposed by Pettijohn et al., 1972. A plot diagram of the major oxide concentration of Log (SiO_2/Al_2O_3) versus Log (Na_2O/K_2O) falling in the field of arkoses, as seen in Figure 5, [22].

5.3.2. Mineralogy

The XRD analysis of Apsara oil field sandstone reservoir shows that show the presence quartz, and variable clay minerals such as plagioclase feldspar, calcite, illite, mica and chlorite as shown in Figure 6. Quartz and plagioclase feldspar presence in this sandstone are the authigenic grains and quartz cementation (overgrowth).

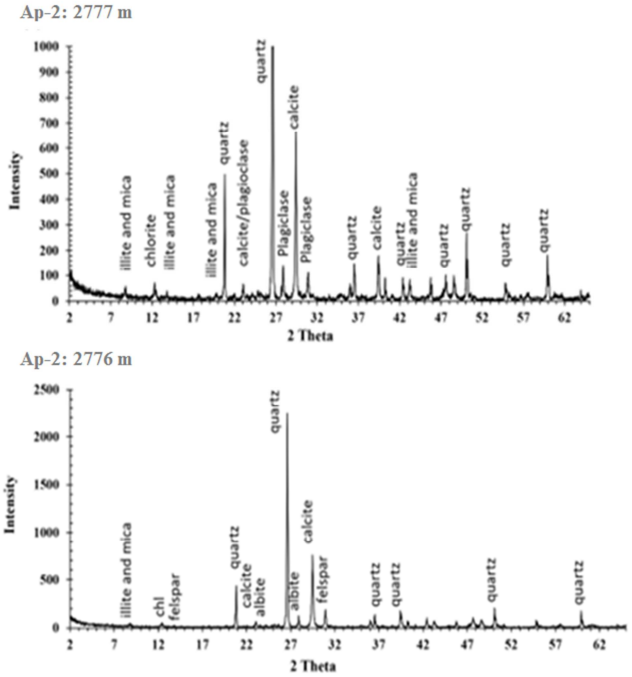

Figure 6. *X-ray diffractograms of Ap-2 at the depth of 2777 m and 2776 m of the Miocene age in Apsara oil field area. The peaks show the presence of minerals in the pore space such as quartz, plagioclase feldspar, calcite, illite, mica and chlorite.*

The clay mineral compositions are the major cementations which accommodated in the pore space in forms of the pore blockage.

In general of Miocene sandstone in the GoT, the more clay minerals the greater reduction of reservoir porosity and permeability [19, 23]. More detailed studies of pore networks are observed additionally the presences of clay mineral types, structures of detrital grains, grain fracturs, mineral recrystallizations, material pore fillings and replacements by Scanning Electron Microscopy (SEM) in the diagenesis

section.

5.4. Porosity and Permeability

The physical porosity of the sandstone reservoir in the study section could be observed pore point counting in the optical images, initiated by Richa et al., (2006) [24].

Based on the visuals of various thin-section and SEM images, pore characteristics on the sample are not homogenized. The skimming of point counts was concluded that optical porosity is ranging below 12% in most cases and occasionally up to 23% with the high grain dissolution images as seen in Figure 7. Thin-section and SEM images presents clearly the pore types, mainly described as grain-grain contact pore, grain fracture pore, and grain dissolution pore which contribute greatly the increasing pore percentage.

Geophysical loggings were interpreted the physical porosity of this section as seen in Figure 2**.** Neuron and density log show that the porosity is 3% to 21%, data interpretation from General Department of Petroleum (GDP), Ministry of Mine and Energy (MME).

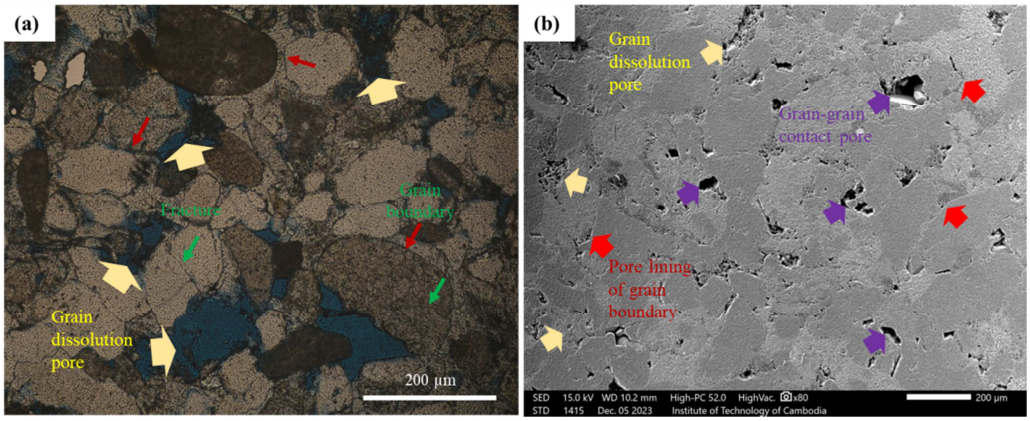

Figure 7. *Pore system observation in the sandstone reservoir rock, at the depth of 2778 m, (a), the thin-section image analysis; (b), the SEM petrographical image.*

The Helium gas injection showed that porosity of sandstone reservoir at the studied depth are below 13%, as seen in Figure 8. The plot diagram of porosity versus depth could be noticed the relation of sandstone porosity to depth layers, basically the greater in depth the lower in pore space Figure 8 (a). Moreover, the permeability measurements were obtained from nitrogen gas flowing through the core samples. Figure 8 (b) shows that the permeabilities are quite low, ranging from 1 to 5 mD and slightly depend on degrees of rock porosity, the more porous rock the better fluid flow or on the other hand, the permeability tends to be lower at deeper layers.

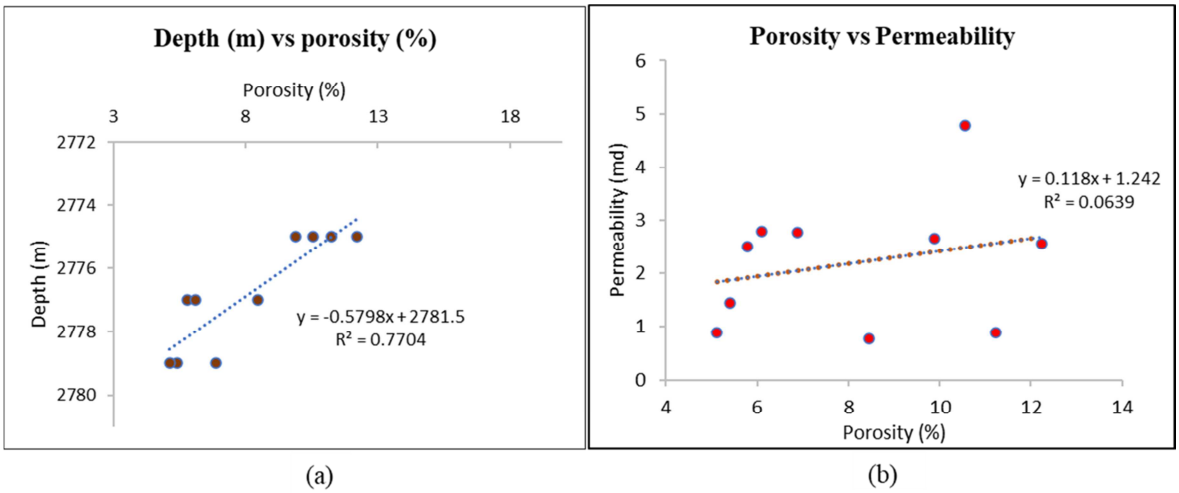

Figure 8. *(a), The plot of the helium gas injection porosity versus the Ap-2 sample depths in the sandstone reservoir section; (b), Plot of the porosity versus permeability (the additional data analysis of porosity and permeability in the plot diagrams are from GDP).*

5.5. Diagenesis

5.5.1. Compaction

Compaction is the weight pressure to become the rock compositions dense and packed which causes by overburden load. Sedimentary rock compaction resulted in rearrangement of the rock detrital grains and changes in the original geometry of grain-grain contacts [25]. As seen in Figure 9 (a), optical image shows polycrystalline lithics bend surround the harder rigid grains (quartz and feldspar), concavo-convex grain

shapes, the presences of fracture on brittle grains Figure 9 (a-b), and the grain-grain contact sutures. These characteristics reveal the evidences of rock layer compaction after it's the sediments had deposited.

In addition, the grain size distribution and rock texture, as seen in the Figure 4 (a-b) and (e) categorized the reservoir zone as fine grain sandstone and grain shorting from inadequately to moderately sorted grains, occasionally containing pebbles, with subangular to subrounded shapes. These typical characteristics of Ap-2 samples are enhancing the process of compaction.

The degree of compaction influences directly to the primary porosity and permeability of the hydrocarbon reservoir rock [26], the most compacted sandstone has very low porosity and permeability.

5.5.2. Cementation and Authigenic Minerals

The cementations are the products of chemically precipitated materials, including new minerals and/ or an addition to an existing mineral to form the cements which bind the grains of sediment together as a typical rock mass.

Based on the XRD analysis, diagram presents the major authigenic minerals such as quartz, calcite, plagioclase feldspar, illite-mica and chloride, as shown in Figure 6. The changes of these mineral due to pore water pressure, sub surface thermal lead to occur the clay cement minerals in the pore spaces of the reservoir rock, as seen clearly by SEM images in Figure 9.

Quart cement could be observed as the quart overgrowth as shown in Figure 9 (a) and (d). This type of cement is reducing the pore spaces at the intergranular pores between surface of quartz grain and other adjacent authigenic grain because quartz cement grows as a continuation of the original quartz grain in accordance with the effective burial and compaction.

Calcite cement was detected in the SEM analysis, as shown in Figure 9 (e). Calcite was original from the carbonate clastic and counted as the framework grain in the rock composition, as seen in Figure 4 (a-b) and Figure 9 (a). Calcite cement generally is the most significant authigenic constituent in the Ap-2 sample of the studied section. This clay cement was investigated likely to situate as grain replacement in the pore network and to block the pore throats.

Illite cements are frequently found in the studied sandstone, presented mostly as hair-like texture, as seen in Figure 9 (f), which occur as pore-filling cement and pore-lining cement.

Chloride cements are rarely seen in the studied samples, however, as shown in Figure 9 (c), the chloride mineral coating takes place on the authigenic material whose recrystallization expose in the micro pores.

The plagioclase feldspar cement is undetectable by the sample analysis; however, feldspar grains are found frequently in the detrital constituent which enhance greatly the secondary porosity in the Apsara oil field reservoir.

The cementations as pore-fillings, pore bride, grain replacement and grain coatings are various in the sample analysis. But the individual clay mineral recognition seems hard to notice, thus, there might be the homogenize of clay mineral mixture in every pore media.

5.5.3. Grain Dissolution

Rock grain dissolution develop the secondary porosity of the reservoir, then, contributing to the total rock porosity higher. According to the sample analysis of this study, feldspar, calcite and cements are the necessary dissolution for improving the rock porosity.

The study of the Pattani Basin sandstone, in the west of the Khmer Basin, find that feldspar dissolution has had a major impact on reservoir quality through the development of secondary porosity by feldspar dissolution and permeability reduction caused by the precipitation of clay mineral in the pore space [19].

Polished section and SEM petrographic offered the evidences of partial and completed dissolution of plagioclase feldspar gain (yellow circle dash), as seen in Figure 9 (a) and (c), respectively. The dissolution pores were replaced by the precipitated minerals which could be identified the partial authigenic growth.

Calcite and/or organic lithic grains were also reported the evidences of their grain dissolution by the study of sandstone reservoir in the GoT. These framework dissolutions such of calcite and lithic fragment are the cement-dissolution porosity. The Calcite cement which corresponded to the dissolution to create the secondary porosity might had formed since the shallow deposition and prevent the diagenesis of compaction. Whenever reaching the dissolution stage, the precipitation mineral to form new calcite cement or the mixture of clay minerals was replaced partially in the intergranular pore, Figure 9 (e).

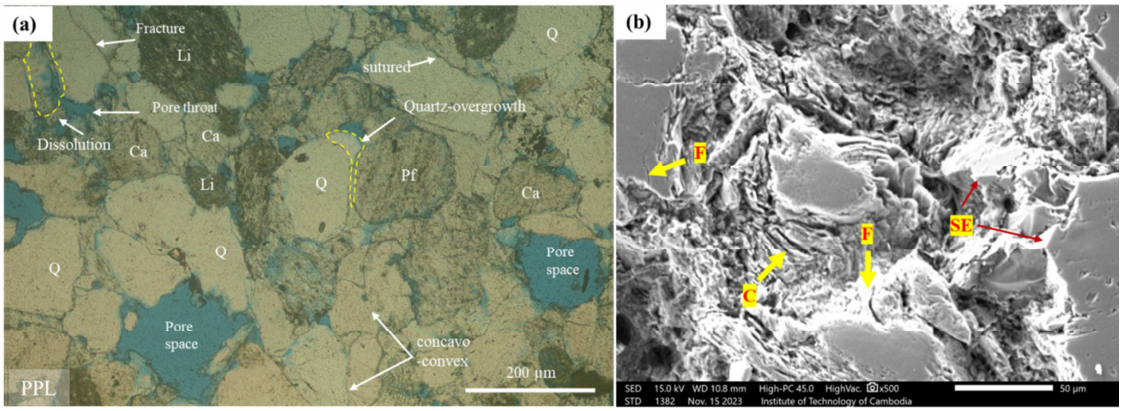

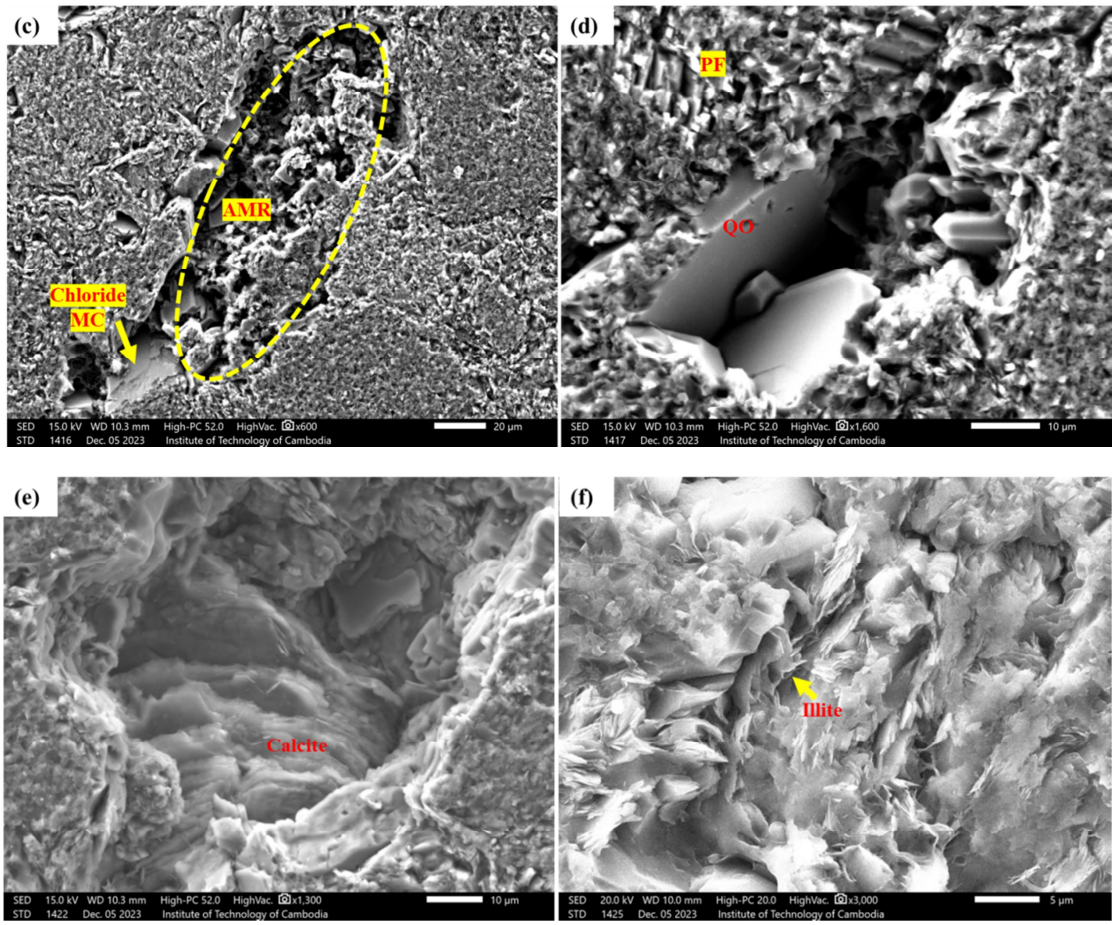

Figure 9. *Petrographical images of the sandstone reservoir in the studied section by polish section and SEM, (a), Thin section image shows the rock components, quartz (Q), lithic fragment (Li), Calcite (Ca), and Plagioclase feldspar (Pf); (b-f), The SEM images of micro composition, calcite (C), fracture (F), serrated edge (SE), Fracture (F), chloride mineral coating (CMC), authigenic mineral replacement (AMR) and quartz overgrowth (QO).*

6. Conclusions

The reservoir section of Apsara oil field area is the interbedding of sand, silty shale with occasional coal through the study of 5 m of Ap-2 core sample, Campex (1993).

These types of interbedding are common in the lithostratigraphy in the Khmer Basin (the information from GDP).

The study of sandstone samples in the age of upper Oligocene to middle Miocene, as of sampling points shown in Figure 3 (a) and (b), geochemistry data determines the arkosic sandstone whose felspathic composition might reach up 25%.

Porosity observations are limited to the similarity in different methods, all of these ranging from 3% to 23%. Point counting in the thin-section petrographs according to size distribution indicates 12% as the maximum porosity (Figure 4 (e)) while lithology logs based on neutron and density shows the porosity ranged from 3% to 23%, as shown in Figure 2. In addition, the helium gas injection method expresses the porosity in range of 4% to 13%, Figure 8. In nature, the sandstone clastic falls into fine to medium grain size and adequately to sub-rounded shape, so the primary porosity and permeability could be defined as low to medium pore sandstone.

Diagenesis mechanism influences extremely the sandstone reservoir characteristic, but very little chances to notice the evidences of reservoir quality improvement which determines the factor controlling reservoir quality in Apsara oil field area.

1) Compaction is noticeably high in the study section due to a high percentage of ductile detrital grain in the rock mass. A greater rounded shape of brittle grain the better swap of ductile material over in the condition of a deep burial depth with high geothermal.
2) Clay minerals and cementation are the keys factors which control the reservoir quality of sandstone reservoir. Quartz overgrowth cement contribute a bigger pore throat blocks which reduce porosity and permeability in this zone. On the other hand, the additional mineral growth in terms of pore bride, pore filling, authigenic replacement and mineral coatings of illite-mica, chloride, calcite, feldspar and a mixture of clay authigenic also reduce the intergranular and intragranular pores and result in the reduction of fluid flow ability.
3) Grain dissolution enhances primarily the rock porosity and permeability, however, the chemical reaction in the presence of pore water pressure and temperature is to form other authigenic materials as a replacement and pore fillings.

The study of sandstone reservoir rock samples in this paper is not possible to reflect the characteristic of the whole reservoir zone from sequence 3 to sequence 4. The scopes of the study have just observed in the 5 meters interval within the

reservoir zone. To have more reliable interpretation of factors control the reservoir quality in this area, sampling points should be taken from all the sand in the potential reservoir zone. In the future work, there might have a study on morphology of mineral recrystallization which impacts on intergranular pore system, and identifies the roles of clay mineral species in the pore throats.

Acknowledgments

This work was funded by Cambodia Higher Education Improvement Project (Credit No. 6221-KH). The authors would also like to thank to General Department of Petroleum (GDP), Ministry of Mines and Energy (MME), Cambodia for providing the core samples and the technical report documents.

Conflicts of Interest

The authors declare no conflicts of interest.

References

[1] J. Blanche and J. Blanche, "An overview of the exploration history and hydrocarbon potential of Cambodia and Laos," 1992.

[2] Q. Rigby, "Living and prospering in an energy hungry world Thailand Cambodia Overlapping Claim Area… Revisited," 2013.

[3] A. Okui, A. Imayoshi, and K. Tsuji, "Petroleum system in the Khmer trough, Cambodia," 1997.

[4] Woodside, "The Prospective and feasibility evaluation for the offshore development base on the discoveries to date and the assessment of economic potential for further exploration in the area.," Technical Report vol. Consultant, 2000.

[5] CNPA, "The case study of Cambodian petroleum sector," *CCOP,* 2003.

[6] CNPA, "Petroleum Sector in Cambodia," *CCOP,* Presentation 2012.

[7] CNPA, "Regional Geology in Khmer Basin," *CCOP,* 2002. [Online]. Available: http://www.ccop.or.th/epf/cambodia/cambodia_us.html.

[8] K. Sokunthea *et al.*, "Reservoir characteristics and production performance forecast using decline curve analysis (DCA) of the five production wells in Apsara field, Cambodia Block A," *SPE,* 2022.

[9] KrisEnergy, "Cambodia's maiden Apsara oil field comes onstream," 2020.

[10] B. Lepic, "KrisEnergy starts up Cambodia's first offshore oil field.," *Offshore Energy,* 2020. [Online]. Available: https://www.offshore-energy.biz/krisenergy-starts-up-cambodias-first-offshore-oil-field/#:~:text=KrisEnergy%20started%20producing%20oil%20from.

[11] KrisEnergy, "Cambodia Block A Production Permit Application, Pimean Akas Area, Apsara Oil Field," 2014.

[12] D. Hubert, G. Kirkwood, and L. Allwright, "Oil Revenue Prospects for Cambodian Economic Analysis of Block A Offshore," *Resources for Development Consulting,* 2015.

[13] A. Pakdeesirote *et al.*, "Horizontal Well Injector/producer Pair Platong Field, Pattani Basin, Thailand," in *Conference on Stratigraphic and Tectonic Evolution of Southeast Asia and the South Pacific (Geothai'97)*, 1997, vol. 19, p. 24.

[14] A. Kornsawan and C. Morley, "The origin and evolution of complex transfer zones (graben shifts) in conjugate fault systems around the Funan Field, Pattani Basin, Gulf of Thailand," *Journal of Structural Geology,* vol. 24, no. 3, pp. 435-449, 2002.

[15] M. B. Fyhn *et al.*, "Palaeocene–early Eocene inversion of the Phuquoc–Kampot Som Basin: SE Asian deformation associated with the suturing of Luconia," *Journal of the Geological Society,* vol. 167, no. 2, pp. 281-295, 2010.

[16] V. Vysotsky, R. Rodnikova, and M. N. Li, "The petroleum geology of Cambodia," *Journal of Petroleum Geology,* vol. 17, no. 2, pp. 195-210, 1994.

[17] K. Neak, K. Kret, T. Sreu, S. Seang, and C. Or, "The Milestone of Cambodian First Oil Production in the Khmer Basin, Gulf of Thailand," *Open Journal of Yangtze Oil and Gas,* vol. 08, no. 02, pp. 19-42, 2023, doi: 10.4236/ojogas.2023.82003.

[18] L. Rigo de Rhigi, J. Baranowski, C. Chaikiturajai, G. Nelson, D. Wechsler, and G. Mattingly, "Block B8/32, Gulf of Thailand petroleum system and implementation of technology in field development," *Seapex Press,* vol. 6, pp. 46-55, 2002.

[19] P. D. Lundegard and A. S. Trevena, "Sandstone diagenesis in the Pattani Basin (Gulf of Thailand): history of water-rock interaction and comparison with the Gulf of Mexico," *Applied Geochemistry,* vol. 5, no. 5-6, pp. 669-685, 1990.

[20] Q. U. Z. Dar *et al.*, "The impact of diagenesis on the reservoir quality of the early Cretaceous Lower Goru sandstones in the Lower Indus Basin, Pakistan," *Journal of Petroleum Exploration and Production Technology,* pp. 1-16, 2022.

[21] P. Chima, C. Baiyegunhi, K. Liu, and O. Gwavava, "Diagenesis and rock properties of sandstones from the Stormberg Group, Karoo Supergroup in the Eastern Cape Province of South Africa," *Open Geosciences,* vol. 10, no. 1, pp. 740-771, 2018.

[22] M. M. Herron, "Geochemical classification of terrigenous sands and shales from core or log data," *Journal of Sedimentary Research,* vol. 58, no. 5, pp. 820-829, 1988.

[23] A. Travena and R. Clark, "Diagenesis of sandstone reservoirs of Pattani Basin," *Gulf of Thailand: AAPG Bulletin,* vol. 70, pp. 299-308, 1986.

[24] Richa, T. Mukerji, G. Mavko, and Y. Keehm, "Image analysis and pattern recognition for porosity estimation from thin sections," in *SEG Technical Program Expanded Abstracts 2006*: Society of Exploration Geophysicists, 2006, pp. 1968-1972.

[25] J. Li, X. Zhang, J. Tian, Q. Liang, and T. Cao, "Effects of deposition and diagenesis on sandstone reservoir quality: A case study of Permian sandstones formed in a braided river sedimentary system, northern Ordos Basin, Northern China," *Journal of Asian Earth Sciences,* vol. 213, p. 104745, 2021.

[26] A. M. Ali and E. Padmanabhan, "Quartz surface morphology of Tertiary rocks from North East Sarawak, Malaysia: Implications for paleo-depositional environment and reservoir rock quality predictions," *Petroleum exploration and development,* vol. 41, no. 6, pp. 761-770, 2014.